Universal electric-field-driven resistive transition in narrow-gap Mott insulators

P. Stoliar,[1,2] L. Cario,[3] E. Janod,[3] B. Corraze,[3]C. Guillot-Deudon,[3]
S. Salmon-Bourmand,[3] V. Guiot,[3] J. Tranchant,[3] M. Rozenberg[1,*]
[1]*Laboratoire de Physique des Solides, CNRS UMR 8502,*
Université Paris Sud, Bât 510, 91405 Orsay, France
[2]*ECyT, Universidad Nacional de San Martín, Campus Miguelete, 1650 San Martín, Argentina and*
[3]*Institut des Matériaux Jean Rouxel (IMN), Université de Nantes,*
CNRS, 2 rue de la Houssinière, BP32229, 44322 Nantes, France

One of today's most exciting research frontier and challenge in condensed matter physics is known as Mottronics, whose goal is to incorporate strong correlation effects into the realm of electronics.[1,2] In fact, taming the Mott insulator-to-metal transition (IMT), which is driven by strong electronic correlation effects, holds the promise of a commutation speed set by a quantum transition, and with negligible power dissipation.[3] In this context, one possible route to control the Mott transition is to electrostatically dope the systems using strong dielectrics, in FET-like devices.[4–6] Another possibility is through resistive switching,[7] that is, to induce the insulator-to-metal transition by strong electric pulsing.[3,8–11] This action brings the correlated system far from equilibrium, rendering the exact treatment of the problem a difficult challenge. Here, we show that existing theoretical predictions of the off-equilibrium manybody problem[12,13] err by orders of magnitudes, when compared to experiments that we performed on three prototypical narrow gap Mott systems $V_{2-x}Cr_xO_3$, $NiS_{2-x}Se_x$ and $GaTa_4Se_8$, and which also demonstrate a striking universality of this Mott resistive transition (MRT). We then introduce and numerically study a model based on key theoretically known physical features of the Mott phenomenon in the Hubbard model.[14] We find that our model predictions are in very good agreement with the observed universal MRT and with a non-trivial timedelay electric pulsing experiment, which we also report. Our study demonstrates that the MRT can be associated to a dynamically directed avalanche.

The resistive transition in Mott insulators is a topic of great current interest in both basic and applied condensed matter physics. On one hand, the understanding of the behavior of a strongly correlated system far from equilibrium remains a formidable many-body physics problem.[12,13,15–19] While on the other hand, it is also a key issue for Mottronics,[1] (i.e., the current challenge of bringing strong correlation effects into the realm of electronics).[2]

The theoretical work on the electric-field-driven breakdown of a Mott state in the Hubbard model is consistent with an intuitive scenario for the onset of the transition.[12,13,15,16,20] In fact, the onset of electric conduction is predicted to occur for a strength of the electric field E_{th} of the order of the Mott-Hubbard gap Δ divided by a length ξ of the order of the unit cell. In a Mott insulator the doublon state, which is the virtual double occupation of a site, is associated to the superexchange interaction, thus extends within distances $\sim \xi$. Then, the electric breakdown due to the deconfinement of the doublon will occur when the field is such that it bends the Hubbard bands by the gap energy Δ within the length ξ. Hence, $E_{th} \sim \Delta/\xi$, so the predicted order of magnitude of the critical field is the order of few V/nm. This is off by several orders of magnitude from the experimental observations, which is typically in the kV/cm (i.e., 10^{-4} V/nm) range.[17,21,22] In addition, and consistent with that observation, the predicted delay time for the transition, that is the time elapsed from the application of the external field till the onset of the conduction jump, is also off with respect to the experimental findings by about three orders of magnitude.[8–11,17,21]

These discrepancies signal a shortcoming of current theoretical approaches to describe the breakdown of Mott insulators by a simple Hubbard model. It is likely, that additional degrees of freedom, such as charge or lattice, may also play a significant role.[17] Evidently, that would add another layer of complexity to the already difficult out-of-equilibrium treatment of the problem. Hence, here we take another approach and shall first show that three different prototypical narrow gap Mott insulators, which all have a pressure driven metal-insulator transition, undergo a universal Mott resistive transition phenomenon. Specifically, they display threshold fields and time delays of similar magnitudes, which are significantly off from theoretical estimates. This surprising finding motivates us to introduce a resistor network model that incorporates basic features known from equilibrium many-body studies of the Mott transition.[14] A similar method was recently used to study current oscillations in VO_2.[23] We study the model by numerical simulations and show that it captures the qualitative behavior observed in experiments. In particular, we find: i) that the MRT may be viewed as a dynamically directed avalanche, and ii) that a new time scale emerges from the local recovery of inhomogeneously transited regions. These observations are further validated by comparison of non-trivial theoretical predictions with experiments of multiple electric pulsing, which we also verify and report.

We study the electric-field-driven MRT in the following selected prototypical three dimensional Mott insulators,[24], $GaTa_4Se_8$, $NiS_{2-x}Se_x$and $V_{2-x}Cr_xO_3$, a ternary and a binary chalcogenide, and an oxide. These compounds are archetypal, as they all undergo an insula-

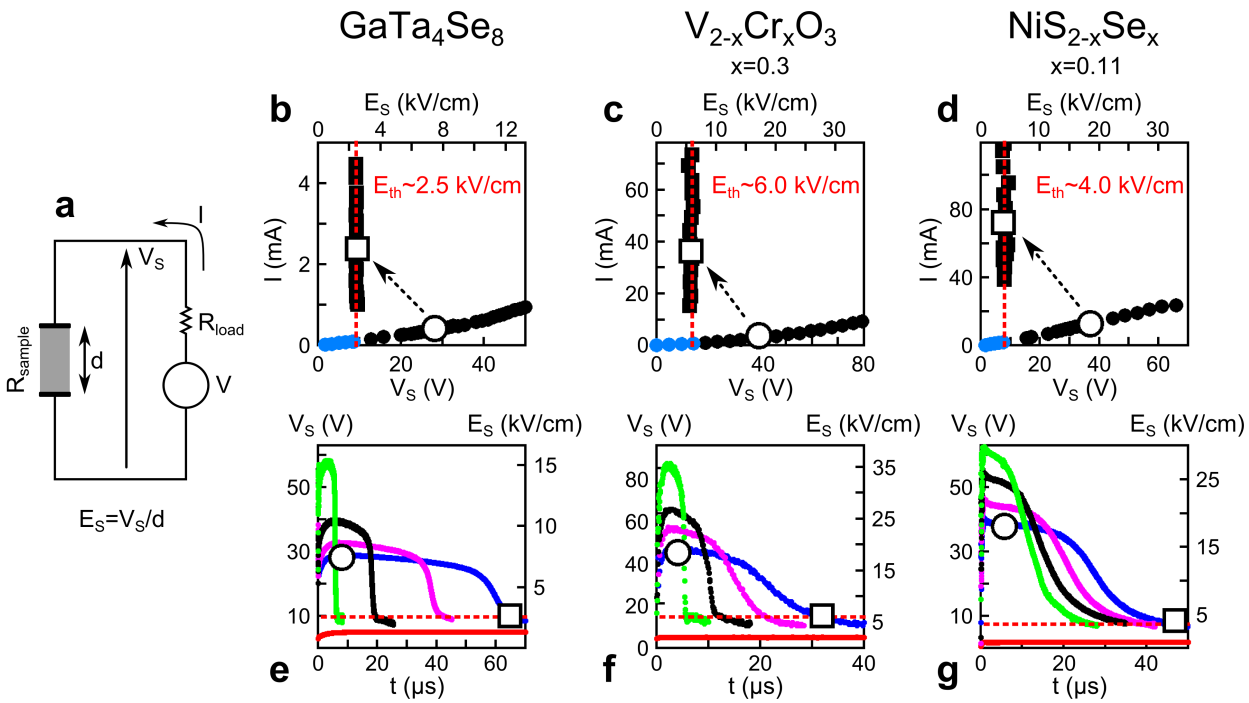

FIG. 1. a) The schematics of the experimental setup. b-g) Universal $I-V$ characteristics (panels b, d, f) and time dependence of the sample voltage $V_S(t)$ (panels c, e, g) for three different types of narrow gap Mott insulators. Blue dots correspond to the region below E_{th}, where no breakdown is observed. Black symbols correspond to the $I-V$ characteristic in the resistive switching region, above E_{th}. The black dots show the initial $I-V$, before the breakdown, and the black squares indicate the final state. The open symbols highlight a particular breakdown transition for easier visualization. Measurements on $GaTa_4Se_8$ were performed at 77 K, on $V_{2-x}Cr_xO_3$ (x=0.3) at 164 K and on $NiSe_{2-x}S_x$ (x=0.11) at 4 K. For further experimental details see the Supporting Information.

tor to metal transition driven by pressure,[24–29] which is in good qualitative agreement with the theoretical predictions of Hubbard model studies in dynamical mean field theory.[14,30] The first compound is actually a representative of a whole family of Mott systems, the AM_4Q_8, with A=Ge, Ga, M=Ta, Nb, V, Mo and Q=Se, S.[25] Notice that an electric-field driven transition has also been reported in VO_2. However, unlike the Mott insulators in the present study does not have a pressure induced transition, but a first order insulator to metal transition driven by increasing temperature.[23,31–34] This is qualitatively different to the present case, since the resistivity of our systems merely shows thermal activated behavior with small gaps of the order of tenths of eV. In Figure 1 we present the $I-V$ curves of the measured resistive transitions of the three Mott systems. They all show similar behavior with a sharp transition onset at an electric field threshold E_{th}. The data also show the delay times for the transition t_d. As mentioned before, the magnitudes of these quantities are off by at least three orders of magnitude from estimates obtained from solutions of Hubbard models.[12,13,15,16] We should also emphasize that the sharp transition is indicative of its electronic origin. In fact, a reduction of resistance due to Joule self-heating would produce and S-shaped $I-V$ characteristic with a gradual evolution of the resistance change.[35]

The resistor network model is schematically shown in Figure 2, where each one of the cells represents a small region of the physical system, which is in either of two well defined electronic states, Mott insulator (MI) or correlated metal (CM). Since the compounds are normally insulators, we assume that the MI-state is lower in energy, which we define as the reference $E_{\rm MI} \equiv 0$. The CM-state is assumed to be a metastable state, with a higher energy $E_{\rm CM}$, and separated from the MI by an energy barrier E_B (see Figure 2). These features are based on previous studies of the Mott-Hubbard transition,[14] that have successfully captured many (equilibrium) properties of this transition.[24,36] Indeed, the dynamical mean field theory studies on the Hubbard model predict the existence of two competing states, very close in energy, which have a region of coexistence close to the first order Mott metal-insulator transition.[14] In our model, the MI and CM states are associated with corresponding high and low resistance values, $R_{\rm MI}$ and $R_{\rm CM}$. The cells are assumed to represent patches of at least a few nanometers in size, such that an electronic state may be well defined. Initially all cells are assumed to be in the MI-state. The time is discretized and the external voltage is applied to the MRN at each timestep. The local voltage

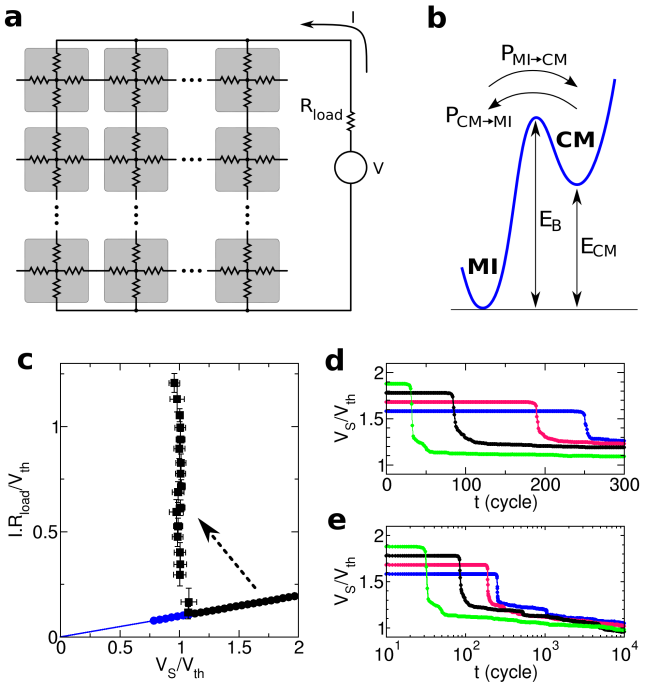

FIG. 2. a) Mott resistor network model and simulation circuit, in analogy with the experimental setup. b) Energy diagram of the CM and MI states and the energy barrier. c) Simulation data of the I-V characteristics, following the same convention as in Fig. 1. d) Time dependence of the sample voltage as a function of simulation time. The data correspond to $V_S/V_{th} = 1.74$, 1.84, 1.95 and 2.06, from right to left. e) Same as panel (d) on semi-log scale to observe the long time behavior.

drops $\Delta V(\mathbf{r})$ are then computed by standard methods.[37] We assume that the MI $\rightarrow$ CM transition rate of each cell is given by $P_{\mathrm{MI}\rightarrow\mathrm{CM}} = \nu\, e^{-(E_B - q\Delta V)/kT}$, where the constant ν is an attempt rate, which we set to unity and similarly the charge q. The precise origin of this transition is not yet fully established. It may be likely driven by injected carrier doping, due to impact ionisation, which could induce the local metalization of a small region.[32,33] However, other mechanisms including electromechanical coupling cannot be ruled out,[38] as Mott insulators may have significant compressibility anomalies near the metal-insulator transition. After a MI $\rightarrow$ CM transition, the metastable CM-state may relax back to the MI by overcoming the energy barrier E_B, with a transition rate given by $P_{\mathrm{CM}\rightarrow\mathrm{MI}} = \nu\, e^{-(E_B - E_{\mathrm{CM}})/kT}$. Notice that, since $R_{\mathrm{MI}} \gg R_{\mathrm{CM}}$, the voltage drop may be neglected in the CM cells. This relaxation process defines an important time scale in the problem, as we shall later see. Under these assumptions, the model can be solved by numerical simulations in discretized time (see Supporting Information for details). In analogy to the experimental setup (see Figure 1), we apply a voltage to the network $V_S = [R_S/(R_S + R_L)]V$, where V is the external voltage, R_S is the equivalent resistance of the network and R_L is a limiting load resistance. Initially, all the cells are in the MI state, and $R_S = R^0_{\mathrm{MI}} = g\, R_{\mathrm{MI}}$, where g is a geometrical factor of the order of unity. Then, during the simulation, the sites may switch between the MI and CM states, and thus the value of R_S is recomputed at every timestep. The specific values of the adopted parameters are detailed in the Supporting information.

As shown in Figure 2, the simulations predict a sharp threshold behavior for the MRT phenomenon and $I-V$ characteristics that are in excellent agreement with the experimental data of Figure 1. Moreover, the simulations also capture the qualitative behavior of the time delay t_d, which increases dramatically as the voltage approaches the threshold from above, and eventually diverges as $V_s \rightarrow V_{th}$.

While one may expect that the sharp threshold stems from a simple percolation process, in fact the simulations unveil a qualitatively different scenario. At low applied V, after an initial transient, the fraction of sites in the CM to those in the MI state stabilizes and is simply given by the ratio between the transition rates $P_{\mathrm{MI}\rightarrow\mathrm{CM}}/P_{\mathrm{CM}\rightarrow\mathrm{MI}}$, which is small since $(E_B - E_{\mathrm{CM}}) < (E_B - \Delta V)$. Beneath the threshold, $\Delta V \approx V/M$, where M is the number of cell layers between the electrodes (see Figure 2). This reflects the equilibrium of concentration condition $N_{\mathrm{MI}} P_{\mathrm{MI}\rightarrow\mathrm{CM}} = N_{\mathrm{CM}} P_{\mathrm{CM}\rightarrow\mathrm{MI}}$.

In a simple percolation picture, the 2D (site) percolation fraction $\sim$0.59 would be reached when the applied voltage is such that $\Delta V \approx E_{\mathrm{CM}}$.[39] However, in our model, already for voltages well beneath that value the MRT takes place in a dynamically directed avalanche phenomenon. The reason may be simply understood. At low $P_{\mathrm{MI}\rightarrow\mathrm{CM}}$ rates (i.e., low applied V), the CM sites are diluted and randomly distributed. However, as V is increased the production rate of CM sites grows, and eventually there is a significant chance of having a few consecutive CM sites longitudinally aligned, in a direction perpendicular to the electrodes. The voltage drop in that low-R_{CM} metallic segment decreases, and induces a compensating increase of the voltage drop at the high-R_{MI} sites that are close to its extremes. Thus, the transition probability MI $\rightarrow$ CM for those sites increase as well, which quickly get added to the metallic segment and further increase the voltage drop at the extremes, eventually leading to a runaway process, or avalanche. This is the dynamically generated directed percolation leading to the MRT. This is visualized in detail in Figure 3, which shows the formation of a conductive path and the enhanced transition probability that develops along the longitudinal direction. Interestingly, this picture is key to understanding many experimental features, and leads to further predictions that we shall test later. In Figure 4, we show the snapshots of the state of the system after a long period of a continuously applied V. Beneath the V_{th} the production of CM sites remains very diluted and far from percolation, with no precursors. From the observation of the panels corresponding to V_S above and below V_{th}, it is clear that the transition occurs for a fraction

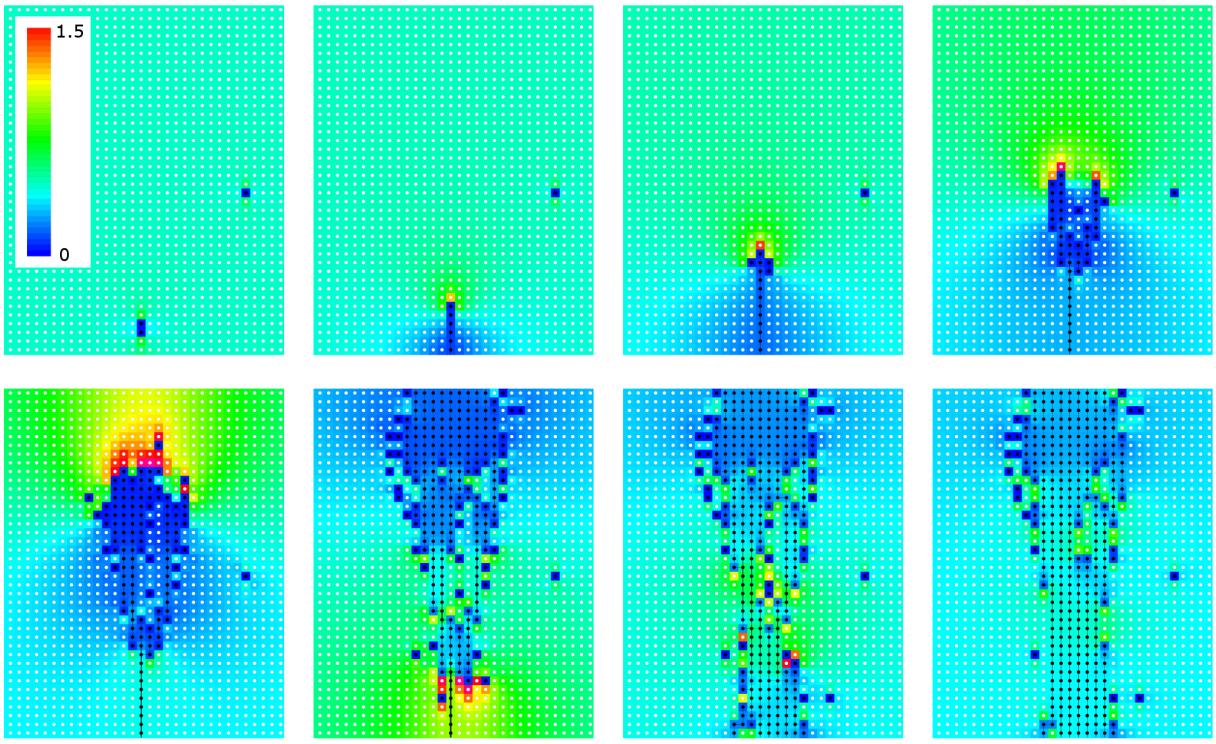

FIG. 3. Intensity color plot of local voltage drops on the resistor network $\Delta V/E_B$. Only the region where the filament forms and the breakdown occurs is shown. The electrodes are at the top and bottom of the panels. The applied voltage is V_S/V_{th} = 1.74, the panes correspond to simulation time t = 60, 70, 75, 80, 83, 85, 87 and 100 (See Supporting Information for the animated data). The state of each cell is represented by a white or a black dot, for MI and CM, respectively.

of CM sites, which is much smaller than the 2D percolation value mentioned before. Above the threshold, quite surprisingly, we observe that the number of conductive paths (or the fraction of the system that is in transited state) increases with the voltage difference to the threshold, $V_S - V_{th}$. We trace this effect to a rapid succession of multiple avalanche events. In fact, after the initial path is formed, so long as the voltage on the sample remains above V_{th}, the avalanche events will continue until the applied voltage on the sample decays down to the value V_{th} (see Figure 2e).

Another interesting prediction of the model is that the low resistance state is not permanent. Since the CM states are metastable, after the applied voltage is switched off, all those sites begin to relax back to the MI state. Thus, Mott resistive transition is, unlike, the permanent dielectric breakdown phenomenon in semiconductors, a volatile effect (i.e., the resistance recovers its original value after the applied voltage is switched off) with a characteristic relaxation time t_{relax} Indeed, experiments reported in the $GaTa_4Se_8$ compound show this sudden recovery effect.[8–11] Therefore, the Mott resistive transition phenomenon is a volatile and fully reversible resistive switching, which is qualitatively different to the nonvolatile resistive switching effect in transition metal oxide systems.[7,40–42]

We finally consider a non-trivial prediction, which follows from the assumptions of our model. Since, one of its key features is relaxation of the CM cells back to the MI state, we may expect a qualitative different behavior if we apply short voltage pulses (i.e., of a duration smaller that the respective t_d), which are repeated at a time interval that may be either shorter or longer than t_{relax}. In fact, since a single pulse is too short to produce the transition, in the case of long time intervals between pulses the effect of each one vanishes due the relaxation before the next pulse arrives. In contrast, if the interval between pulses is shorter than t_{relax}, then the effect of successive pulses will accumulate, and eventually drive the transition. In Figure 5 we show the theoretical prediction along with the respective experimental data in the $GaTa_4Se_8$ Mott insulator. An excellent qualitative agreement is observed, which provides a definite nontrivial validation of our model.

In conclusion, we found universal behavior in electric field-induced insulator-to-metal transition experiments of various prototypical narrow-gap Mott insulator compounds, $V_{2-x}Cr_xO_3$, $NiS_{2-x}Se_x$ and $GaTa_4Se_8$. These features motivated the formulation of a resistor network model, which we studied numerically. We obtained excellent agreement with the experimental data, and also with a non-trivial delayed voltage pulsing experiment predicted by the model. The numerical simulations showed that the physical origin of the Mott resistive transition is

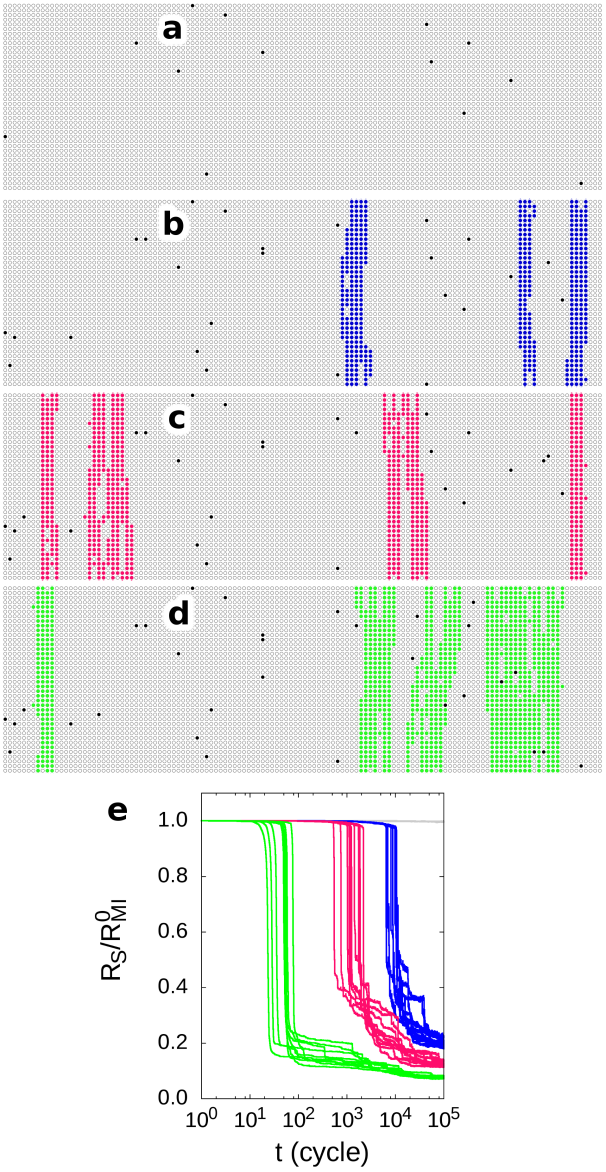

FIG. 4. Local resistance snapshot of the network after a long simulation time of 10^5 cycles. The black and color dots indicate the sites that are in the CM state, while the grey dots correspond to the sites in the MI state. The dots forming filaments are coloured for easier visualization. The initially applied sample voltage were V_S/V_{th} = 0.7, 1.1, 1.4 and 1.8 (panels (a) to (d)). The right panel (e) shows the dependence of the normalized network resistance ($R_S/R^0_{\rm MI}$), as a function of simulation time. The color notation is as in the previous panels. The dispersion of the data corresponds to 10 runs with different seeds, which illustrate the effect of the finite size of the network.

a dynamically directed avalanche mechanism. Our study brings new insight to the difficult problem of the behavior of Mott systems out of equilibrium, and is a timely stepping-stone for research in the emerging field of Mottronic devices.

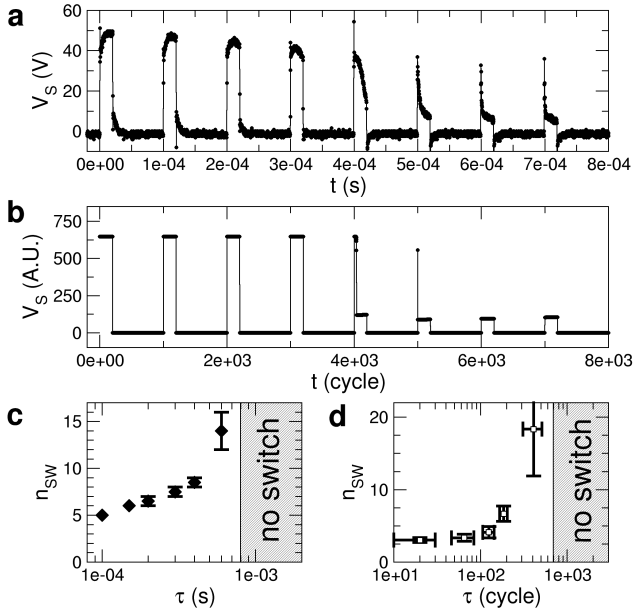

FIG. 5. Electric pulsing with varying pulse-interval time. a) Sample voltage V_S as a function of time of a $GaTa_4Se_8$-based device upon the application of a train of voltage pulses of 60 V and duration of 20 μs with a period τ=100 μs. Notice that for a continuously applied voltage of 60 V, the device switches after a delay time of $t_d = 70\mu$s (see Supporting Information). b) Simulation data for a train pulse showing the same qualitative behavior. c) Experimental number of pulses required for switching as a function of the pulse period. The pulse duration is as in (a). The grey area corresponds to a pulse-interval where switching no longer occurs. It indicates that the $t_{relax} \sim 800\mu s$. d) Simulation results for varying the pulse-interval. Error bars are due to finite size effects.

ACKNOWLEDGMENTS

This work was supported by the French Agence Nationale de la Recherche through the funding of the "NanoMott" (ANR-09-Blan-0154-01) and "Mott-RAM" (ANR-2011-EMMA-016-01) projects. The authors acknowledge Prof. Aharon Kapitulnik, Prof. D. Roditchev, Dr T. Cren and Dr V. Ta Phuoc for useful discussions.

[1] I. H. Inoue and M. J. Rozenberg, Adv. Funct. Mater. **18**, 2289 (2008).
[2] H. Y. Hwang, Y. Iwasa, M. Kawasaki, B. Keimer, N. Nagaosa, and Y. Tokura, Nat Mater **11**, 103 (2012).
[3] "International technology roadmap for semiconductors," http://www.itrs.net/ (2011).
[4] H. Takagi and H. Y. Hwang, Science **327**, 1601 (2010).

[5] M. Nakano, K. Shibuya, D. Okuyama, T. Hatano, S. Ono, M. Kawasaki, Y. Iwasa, and Y. Tokura, Nature **487**, 459 (2012).

[6] S. Asanuma, P.-H. Xiang, H. Yamada, H. Sato, I. H. Inoue, H. Akoh, A. Sawa, K. Ueno, H. Shimotani, H. Yuan, M. Kawasaki, and Y. Iwasa, Appl. Phys. Lett. **97**, 142110 (2010).

[7] M. Rozenberg, Scholarpedia **6**, 11414 (2011).

[8] L. Cario, C. Vaju, B. Corraze, V. Guiot, and E. Janod, Adv. Mater. **22**, 5193 (2010).

[9] E. Souchier, L. Cario, B. Corraze, P. Moreau, P. Mazoyer, C. Estournès, R. Retoux, E. Janod, and M.-P. Besland, Phys. Status Solidi RRL **5**, 53 (2011).

[10] J. Tranchant, E. Janod, L. Cario, B. Corraze, E. Souchier, J.-L. Leclercq, P. Cremillieu, P. Moreau, and M.-P. Besland, *EMRS 2012 Symposium L*, Thin Solid Films **533**, 61 (2013).

[11] C. Vaju, L. Cario, B. Corraze, E. Janod, V. Dubost, T. Cren, D. Roditchev, D. Braithwaite, and O. Chauvet, Microelectron. Eng. **85**, 2430 (2008).

[12] T. Oka and H. Aoki, Phys. Rev. B **81**, 033103 (2010).

[13] F. Heidrich-Meisner, I. González, K. A. Al-Hassanieh, A. E. Feiguin, M. J. Rozenberg, and E. Dagotto, Phys. Rev. B **82**, 205110 (2010).

[14] A. Georges, G. Kotliar, W. Krauth, and M. J. Rozenberg, Rev. Mod. Phys. **68**, 13 (1996).

[15] T. Oka, R. Arita, and H. Aoki, Phys. Rev. Lett. **91**, 066406 (2003).

[16] T. Oka and H. Aoki, Phys. Rev. Lett. **95**, 137601 (2005).

[17] Y. Taguchi, T. Matsumoto, and Y. Tokura, Phys. Rev. B **62**, 7015 (2000).

[18] S. Dutta, S. Lakshmi, and S. K. Pati, J. Phys.: Condens. Matter **19**, 322201 (2007).

[19] M. Eckstein, T. Oka, and P. Werner, Phys. Rev. Lett. **105**, 146404 (2010).

[20] C. H. Ahn, A. Bhattacharya, M. Di Ventra, J. N. Eckstein, C. D. Frisbie, M. E. Gershenson, A. M. Goldman, I. H. Inoue, J. Mannhart, A. J. Millis, A. F. Morpurgo, D. Natelson, and J.-M. Triscone, Rev. Mod. Phys. **78**, 1185 (2006).

[21] C. Vaju, L. Cario, B. Corraze, E. Janod, V. Dubost, T. Cren, D. Roditchev, D. Braithwaite, and O. Chauvet, Adv. Mater. **20**, 2760 (2008).

[22] F. Sabeth, T. Iimori, and N. Ohta, *Journal of the American Chemical Society*, J. Am. Chem. Soc. **134**, 6984 (2012).

[23] T. Driscoll, J. Quinn, M. Di Ventra, D. N. Basov, G. Seo, Y.-W. Lee, H.-T. Kim, and D. R. Smith, Phys. Rev. B **86**, 094203 (2012).

[24] M. Imada, A. Fujimori, and Y. Tokura, Rev. Mod. Phys. **70**, 1039 (1998).

[25] R. Pocha, D. Johrendt, B. Ni, and M. M. Abd-Elmeguid, *Journal of the American Chemical Society*, J. Am. Chem. Soc. **127**, 8732 (2005).

[26] E. Dorolti, L. Cario, B. Corraze, E. Janod, C. Vaju, H.-J. Koo, E. Kan, and M.-H. Whangbo, *Journal of the American Chemical Society*, J. Am. Chem. Soc. **132**, 5704 (2010).

[27] V. Guiot, E. Janod, B. Corraze, and L. Cario, Chem. Mater. **23**, 2611 (2011).

[28] S. Miyasaka, H. Takagi, Y. Sekine, H. Takahashi, N. Môri, and R. J. Cava, J. Phys. Soc. Jpn. **69**, 3166 (2000).

[29] V. Ta Phuoc, C. Vaju, B. Corraze, R. Sopracase, A. Perucchi, C. Marini, P. Postorino, M. Chligui, S. Lupi, E. Janod, and L. Cario, Phys. Rev. Lett. **110**, 037401 (2013).

[30] G. Kotliar and D. Vollhardt, Physics Today **57**, 53 (2004).

[31] H.-T. Kim, B.-J. Kim, S. Choi, B.-G. Chae, Y. W. Lee, T. Driscoll, M. M. Qazilbash, and D. N. Basov, J. Appl. Phys. **107**, 023702 (2010).

[32] H.-T. Kim, B.-G. Chae, D.-H. Youn, S.-L. Maeng, G. Kim, K.-Y. Kang, and Y.-S. Lim, New Journal of Physics **6**, 52 (2004).

[33] V. Guiot, L. Cario, E. Janod, B. Corraze, V. Ta Phuoc, M. Rozenberg, P. Stoliar, T. Cren, and D. Roditchev, Nat Commun **4**, 1722 (2013).

[34] A. Zimmers, L. Aigouy, M. Mortier, A. Sharoni, S. Wang, K. G. West, J. G. Ramirez, and I. K. Schuller, Phys. Rev. Lett. **110**, 056601 (2013).

[35] B. K. Ridley, Proceedings of the Physical Society **82**, 954 (1963).

[36] P. Limelette, A. Georges, D. Jérome, P. Wzietek, P. Metcalf, and J. M. Honig, Science **302**, 89 (2003).

[37] S. Kirkpatrick, Rev. Mod. Phys. **45**, 574 (1973).

[38] V. Dubost, T. Cren, C. Vaju, L. Cario, B. Corraze, E. Janod, F. Debontridder, and D. Roditchev, Adv. Funct. Mater. **19**, 2800 (2009).

[39] D. Stauffer and A. Aharony, *Introduction To Percolation Theory* (Taylor & Francis, 1992).

[40] A. Sawa, Materials Today **11**, 28 (2008).

[41] R. Waser, R. Dittmann, G. Staikov, and K. Szot, Adv. Mater. **21**, 2632 (2009).

[42] Y. V. Pershin and M. Di Ventra, *Advances in Physics*, Advances in Physics **60**, 145 (2011).